

One-DoF robust control of shaft supported magnetically

ZDZISŁAW GOSIEWSKI and ARKADIUSZ MYSTKOWSKI

The paper presents a robust control of the motion of a shaft supported by magnetic bearings. The dynamics of magnetic suspension systems are characterized by their instability and uncertainty of the plant. Therefore apart from the model of the plant we determined a model of the parametrical uncertainty. The uncertainty is modeled as additive. Current stiffness k_i and displacement stiffness k_s are assumed to be the uncertainty parameters. The performance of the closed-loop system, signals limits, and the disturbances influence are determined with the aid of the weighting functions. Three weighting functions are designed: $W_e(s)$ —penalizing the error signal e , $W_u(s)$ —penalizing the input signal u , and $W_y(s)$ —penalizing the output signal x . For these functions and the uncertainty model we assigned the augmented control model. For the augmented control system we assigned the robust controller. The robust controller assures high quality of control despite of the uncertainty model of the plant, disturbances in the systems, signals limits and high dynamics of the system. Next the H_∞ closed-loop system is compared with the standard PID closed-loop system. Finally simulation results show effectiveness of the control system as good initial responses/transient responses and robustness of the designed robust controller.

Key words: active magnetic bearings (AMB), robust controller, weighting functions, H_∞ norm

1. Introduction

The active magnetic suspension system enable for non-contact suspension of shaft [6]. That means no friction forces and no mechanic wear in kinematical pair. Standard control methods do not allow us to take into account the all factors which influence on static and dynamic quality of control. Thus, in the paper we consider the robust control. The robust control allows us to achieve a good control performances in spite of disturbances and uncertainty of plant. Particularly the robust control method can be used to control of nonlinear and unstable systems [7]. The signals limits can also be consider in the robust stable system. In the paper the robust control was applied in the magnetic bearings system.

The Authors are with Technical University of Bialystok, Mechanical Department, Wiejska 45C, 15-351 Bialystok, e-mail: mystek@pb.bialystok.pl

Received 8.11.2005. Revised 27.02.2006.

In our considerations we assumed that the rigid rotor was supported in two radial magnetic bearings and one axial bearing [3]. Each of the radial bearings limit motion of the rotor in two directions. Such system has five degrees of freedom (5-DoF). We assumed that the control system can be designed independently for each of control directions. The mass of the rotor was reduced to bearing planes. It means, we have omitted coupling effects between particular degrees of freedom. Thus, we will design control loop for each degree of freedom (one-DoF control). Such approach is fully justified for slowly rotating rotor. In this work the plant model and the uncertainty model of the plant was showed. The PID controller was also designed. The PID controller was used to stabilize nominal model of unstable open-loop system. In the augmented system we considered the additive uncertainty model. The performances of the closed-loop system were defined. The constraints of input and output signals are described by the weighting functions. For robust control purpose the weighting functions were designed.

2. Plant of control

The plant of control is a rotor suspended in the electromagnetic field by two radial magnetic bearings. The open-loop model of magnetic bearings system for each axis of control is given by the following model [3]:

$$\begin{aligned} \dot{x} &= A_c x + B_c u, \\ y &= Cx, \end{aligned} \tag{1}$$

where:

$$A_c = \begin{bmatrix} 0 & 1 & 0 & 0 \\ v_1 & 0 & v_{21} & -v_{22} \\ 0 & -v_{31} & -v_{41} & 0 \\ 0 & v_{32} & 0 & -v_{42} \end{bmatrix}, \quad B_c = \begin{bmatrix} 0 & 0 \\ 0 & 0 \\ v_{51} & 0 \\ 0 & v_{52} \end{bmatrix}, \quad C = I, \quad x = \begin{bmatrix} x \\ \dot{x} \\ i_1 \\ i_2 \end{bmatrix}, \quad u = \begin{bmatrix} u_1 \\ u_2 \end{bmatrix}$$

$$v_1 = \frac{k_{s1} + k_{s2}}{m_r}, \quad v_{21} = \frac{k_{i1} + k_{i2}}{m_r} \frac{x_0 + x_z}{2x_0}, \quad v_{22} = \frac{k_{i1} + k_{i2}}{m_r} \frac{x_0 - x_z}{2x_0},$$

$$v_{31} = \frac{k_{i1}}{L_{s1} + L_{01}}, \quad v_{32} = \frac{k_{i2}}{L_{s2} + L_{02}},$$

$$v_{41} = \frac{R_1}{L_{s1} + L_{01}}, \quad v_{42} = \frac{R_2}{L_{s2} + L_{02}}, \quad v_{51} = \frac{k_{w1}}{L_{s1} + L_{01}}, \quad v_{52} = \frac{k_{w2}}{L_{s2} + L_{02}},$$

x_0 —air gap [m], x_z —mass displacement of shaft from centre of magnetic bearing to operating point [m], K —design constant of magnetic bearing, u —voltages [V], R —resistance of coils [Ω], L_s , L_0 —losses inductance and inductances of air gap [H], k_i —current stiffness [N/A], k_s —displacement stiffness [N/m], m —mass of rotor reduced to bearing plane [kg],

A –radial surface of pole piece [m^2], N –number of coils. The index $\{1\}$ and $\{2\}$ describes upper and lower coils.

The operating point is described by the parameters given as follows:

$$x = x_z, \quad i_{z1} = \frac{x_0 - x_z}{x_0} i_0, \quad i_{z2} = \frac{x_0 + x_z}{x_0} i_0. \quad (2)$$

The linear model of plant is described by the following transfer function [3]:

$$G(s) = \frac{\frac{2k_i}{m}}{(L_s + L_0)s^3 + Rs^2 + \left(L_0 \frac{2k_s}{m} - (L_s + L_0) \frac{2k_s}{m} \right) s - R \frac{2k_s}{m}}. \quad (3)$$

2.1. Nominal model of the plant

The model of the plant with nominal parameters is called nominal model. The values of nominal parameters are calculated for some operating point. The nominal model has to reflect the real plant as exactly as possible. The magnitude of the uncertainty model should be smaller. When the model of the plant corresponds to the real plant, the magnitude of the uncertainty model is small. In our case the best nominal model is for operating point: $x_z = 0$.

We assumed that uncertain parameters are: k_i and k_s . In our case the nominal values of k_i and k_s are: $k_i = 280 \text{ N/A}$ and $k_s = 2.3 \cdot 10^6 \text{ N/m}$. For the following nominal data: $m = 22 \text{ kg}$, $R = 0.5 \Omega$, $L_s = 0 \text{ H}$, $L_0 = 0.05 \text{ H}$, the nominal model of plant (for $L_s = 0$) is given by the model:

$$G_0(s) = \frac{25.45}{0.05s^3 + 0.5s^2 - 104545.45}. \quad (4)$$

Fig. 1 shows the simulation scheme for the nominal model one-DoF active magnetic suspension.

3. Design of model uncertainty in magnetic bearings system

The robust controller should assure good performance in the case when the nominal model does not exactly reflects the real plant. Because the states of process controll are time-variant, the uncertainty model is needed. Also when external disturbances have high dynamic (wide frequency spectrum) the uncertainty model is necessary. The robust control with uncertainty modelling is especially useful when parameters of the real plant are variable.

3.1. Parametric uncertainty

For robust control purposes we have to define how nominal model differs from the real plant at particular frequencies. We also have to assure a required bandwidth. The size

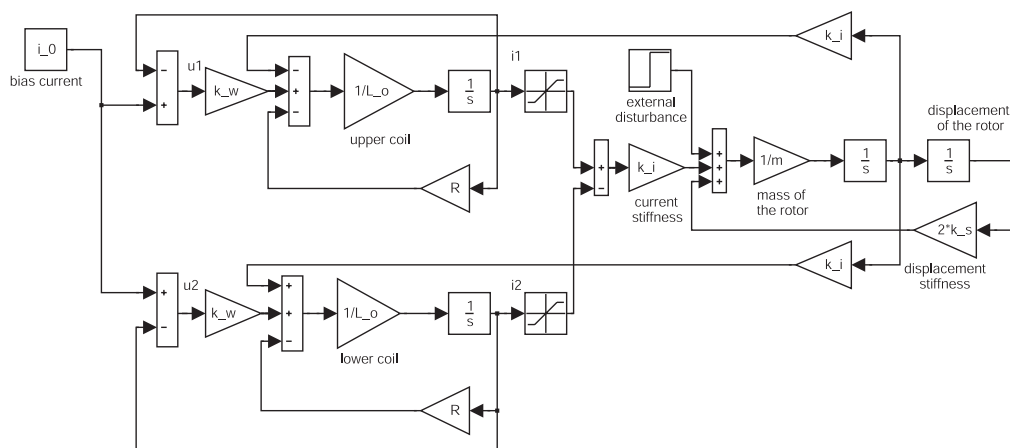


Figure 1. The nominal model of active magnetic suspension

of the model variation is defined by the uncertainty of parameters. Different positions of shaft x_z in air gap cause changes of the induction in upper and lower coils. These inductions are described as follows [3]:

$$L_{01} = \frac{K_1}{2(x_0 - x_z)}, \quad L_{02} = \frac{K_2}{2(x_0 - x_z)}, \quad (5)$$

The nominal values of parameters k_i and k_s are given in the form:

$$k_i = \frac{K}{2} \frac{i_0}{x_0^2} = L_0 \frac{i_0}{x_0^2}, \quad k_s = \frac{K}{2} \frac{i_0^2}{x_0^3} = L_0 \frac{i_0^2}{x_0^3}. \quad (6)$$

The ranges of uncertain parameters are shown in Tab. 3.1. The deviation of parameters was calculated for the case when the shaft rests on the safety bearings ($x_z = 0.5x_0$).

Parameter	Nominal value	Deviation	
		Min	Max
x_0 [m]	$0.5 \cdot 10^{-3}$	$-0.25 \cdot 10^{-3}$	$0.25 \cdot 10^{-3}$
L_0 [H]	0.05	0.03	0.1
k_i [N/A]	280	162	540
k_s [N/m]	$2.3 \cdot 10^6$	$0.8 \cdot 10^6$	$2.9 \cdot 10^6$

Table 2. The values of uncertain parameters

For minimum and maximum values of uncertain parameters, the model of the plant is given by the following equations:

$$G(s)_{\min} = \frac{14.7}{0.05s^3 + 0.5s^2 - 36364}, \quad G(s)_{\max} = \frac{49}{0.05s^3 + 0.5s^2 - 131820}. \quad (7)$$

Fig. 2 shows amplitude-frequency plots of the nominal plant and of the plant with uncertain parameters k_i and k_s .

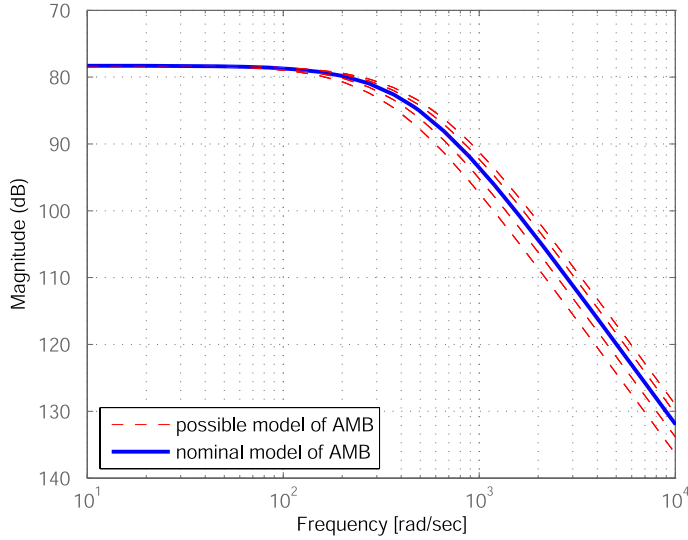


Figure 2. Amplitude-frequency characteristics of the nominal plant and for the plant with uncertain parameters k_i and k_s

The uncertainties of parameters k_i and k_s are given as follows [11]:

$$\begin{aligned} k_i &= k_{i0} + W_{k_i} \delta_i, \quad \text{for } |\delta_i| \leq 1, \\ k_s &= k_{s0} + W_{k_s} \delta_s, \quad \text{for } |\delta_s| \leq 1, \end{aligned} \quad (8)$$

where: k_{i0} , k_{s0} —nominal values of parameters k_i and k_s , W_{k_i} , W_{k_s} —weighting functions of uncertain parameters k_i and k_s , respectively.

3.2. Additive uncertainty

For the nominal model of the magnetic bearings system described by equation (3), the model of additive uncertainty is given by follows [11]:

$$\Delta_a(s) = G(s) - G_0(s). \quad (9)$$

The frequency information about the additive uncertainty model is needed. The spectral transfer function of the additive uncertainty is given by inequality:

$$|\Delta_a(j\omega)| = |G(j\omega) - G_0(j\omega)| \leq l_a(j\omega), \quad \forall \omega. \quad (10)$$

The maximum value of the additive uncertainty is limited by the boundary function $l_a(j\omega)$. Fig. 3 shows the amplitude-frequency characteristics of the additive uncertainty function $\Delta_a(j\omega)$ and of the boundary function $l_a(j\omega)$.

The simulation model of the H_∞ closed-loop system with the additive uncertainty is presented in Fig. 4.

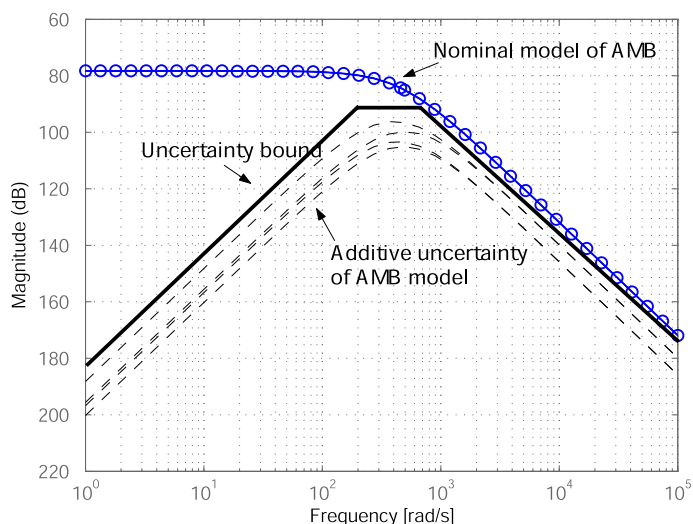


Figure 3. Amplitude-frequency plots of the plant nominal model, additive uncertainty $\Delta_a(j\omega)$ and boundary function $I_a(j\omega)$

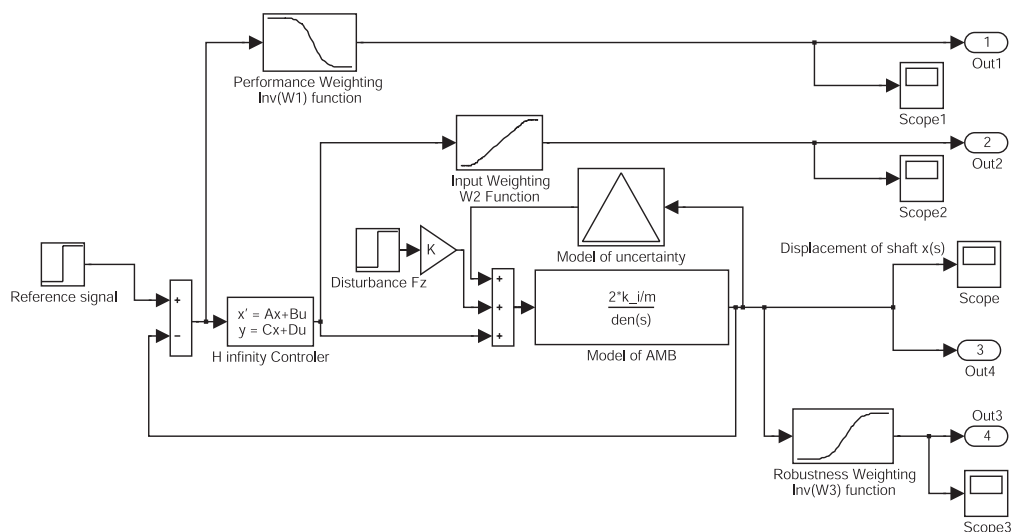


Figure 4. Simulation model of the H_∞ closed-loop system with the additive uncertainty

4. Design process of control system

4.1. Weighting functions

The performance of the robust control system depends on the properly chosen weighting functions. The weighting functions describe the influence of particularly signals on the control system behaviour. The proper choose of the weighting functions is

important. The input weighting function $W_u(s)$, the robustness weighting function $W_y(s)$ and the performance weighting function $W_e(s)$ were designed. They have the form:

$$\begin{aligned} W_e(s) &= \frac{0.33s^2 + 577.4s + 250000}{s^2 + 100s + 2500}, \\ W_y(s) &= \frac{10s + 30000}{s + 60000}, \\ W_u(s) &= \frac{s + 666.7}{0.01s + 1000}. \end{aligned} \quad (11)$$

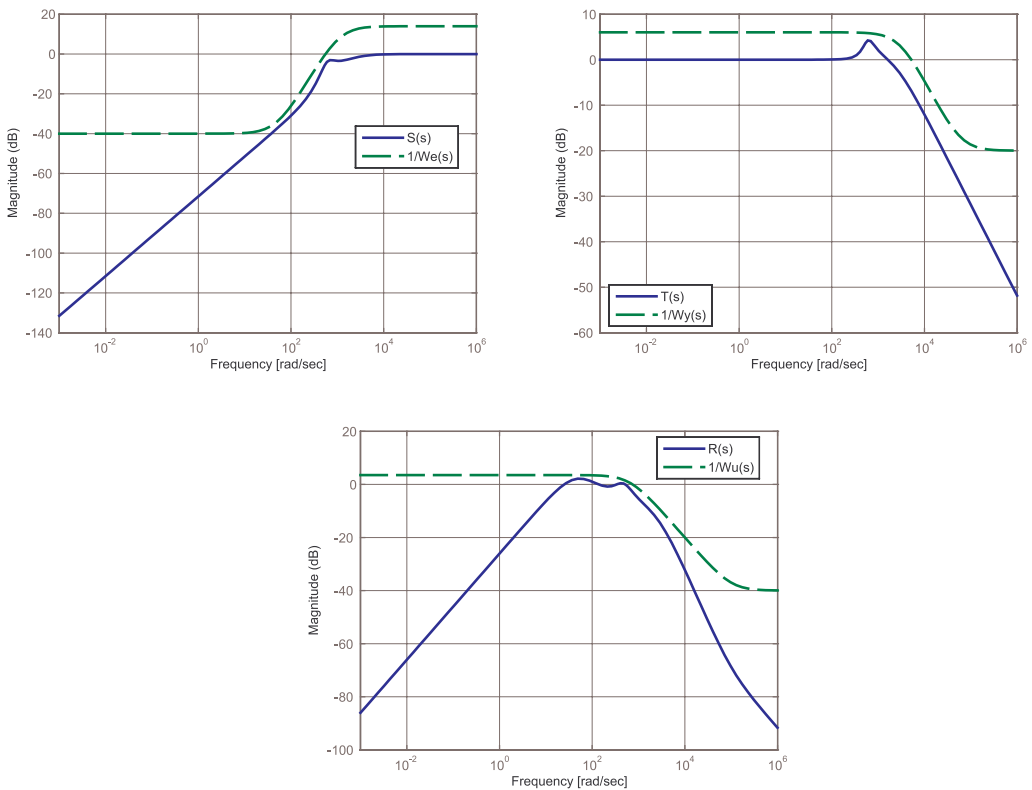


Figure 5. Amplitude-frequency plots of the weighting functions: $W_u(s)$, $W_e(s)$ and $W_y(s)$

The robustness function $W_y(s)$ was designed basing on the sensitivity function $S(s) = (I + G_0(s)K(s))^{-1}$. The input function $W_u(s)$ was assigned basing on the control function $R(s) = K(s)(I + G_0(s)K(s))^{-1}$. The performance function $W_e(s)$ was selected using the complementary sensitivity function $T(s) = G_0(s)K(s)S(s)$. Fig. 5 shows the amplitude-frequency plots of the weighting functions. The simulation model of the H_∞ closed-loop system with the weighting functions is given in Fig. 6. Fig. 7 presents the amplitude-

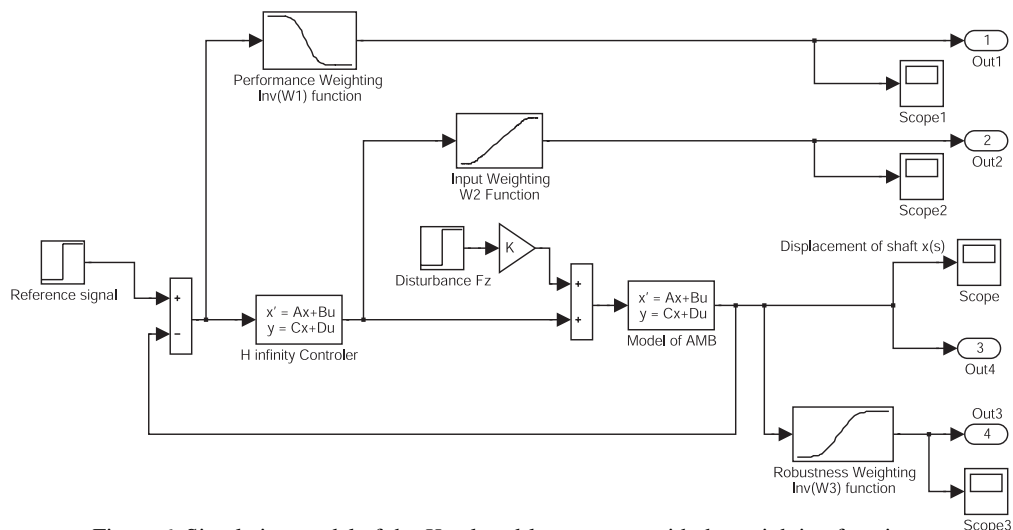


Figure 6. Simulation model of the H_∞ closed-loop system with the weighting functions

frequency characteristics of the functions: $S(s)$ and $T(s)$ for the uncertainty of the plant.

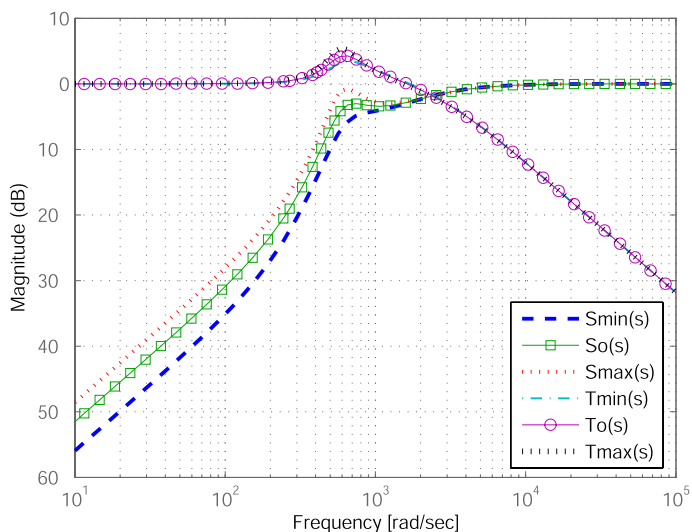


Figure 7. Amplitude-frequency plots of the functions: $S(s)$ and $T(s)$

The weighting functions limit the output and input signals of the control system. The output signal (displacement of the shaft) is limited to 50% of the air gap $x_0 = 0.5$ mm. The input signal (current control) is limited to 10 A. The current control signals in upper and lower coils of the magnetic bearings are shown in Fig. 8. The step load force $F = 800$ N is a disturbance signal.

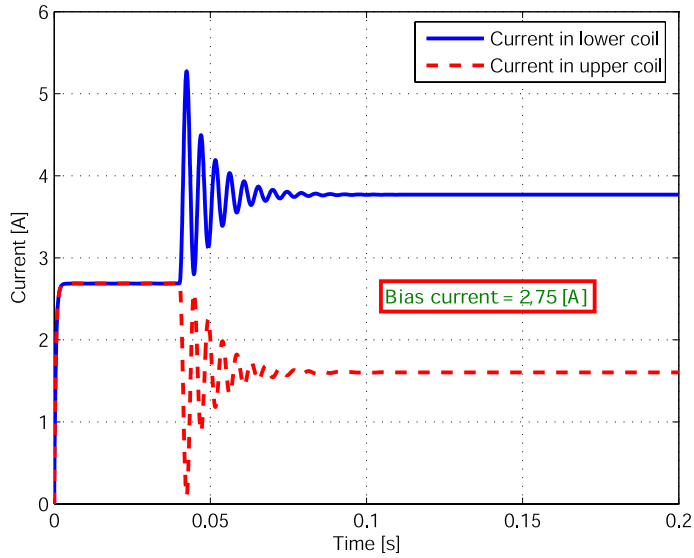


Figure 8. Current control signals in upper and lower coils of the magnetic bearings for step disturbance force $F = 800\text{N}$

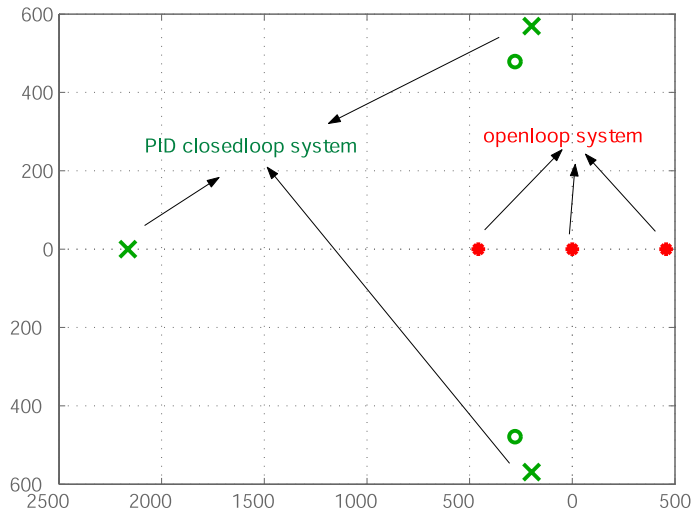


Figure 9. Pole-maps of the closed-loop and the open-loop systems

4.2. Desing process of the PID controller

The design process of the robust controller bases on the nominal closed-loop system with PID controller. For magnetic suspension system we have designed PID controller

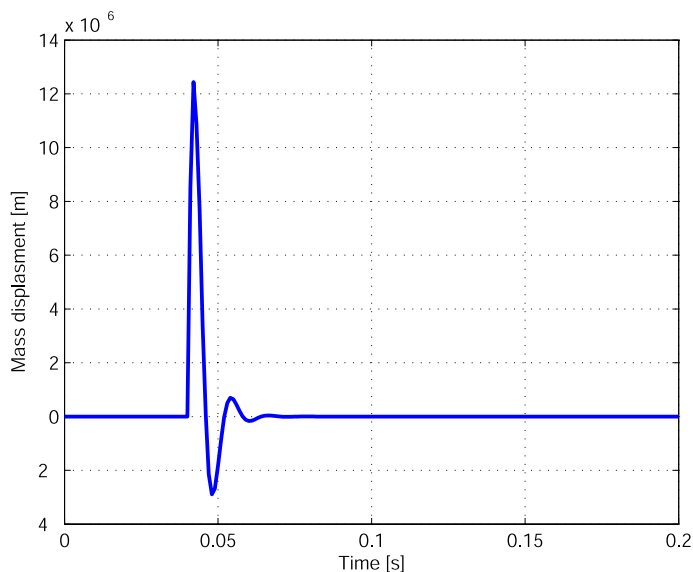


Figure 10. Step response of the PID closed-loop system for input force $F = 600\text{N}$

which is given by the following transfer function:

$$K(s) = \frac{100.6s^2 + 56150s + 30900000}{s} \quad (12)$$

The pole-maps of the open-loop system and the PID closed-loop system are shown in Fig. 9. The displacement of the shaft for the input step force $F = 600\text{N}$ is presented in Fig. 10.

4.3. Design process of the H_∞ controller

The robust control problem is to find stable controller K , which minimalizes the following norm [1]: $\|F(G, K)\|_\infty = \sup_{\omega \in \mathcal{R}} |F(G, K)(j\omega)|$, where $F(G, K)$ is the transfer function of the closed-loop system. The diagram of the standard robust closed-loop system is shown in Fig. 11. To obtain the robust controller a design process of the augmented model is necessary. The augmented model includes model of the plant and the weighting functions. In case of the robust control H_∞ the problem is to find controller K that fulfills the following condition [2]:

$$\|F(G, K)\|_\infty < \gamma, \quad (13)$$

where γ is a minimal value of optimization factor.

The stability condition of the robust closed-loop system is described as follows [2]:

$$\forall \Delta \in H_\infty, \quad \|r^{-1}\Delta\|_\infty < 1 \quad \text{if} \quad \|rF(P, K)\|_\infty \leq 1, \quad (14)$$

where r is the boundary function of the uncertainty function and: $\|\Delta(j\omega)\| < r(j\omega)$.

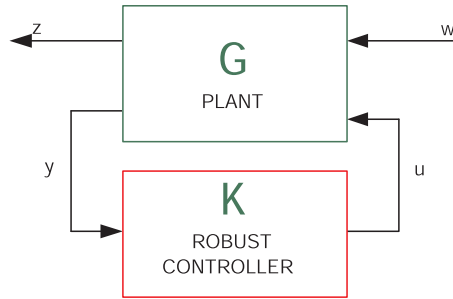


Figure 11. Diagram of the robust closed-loop system: w –reference signal, u –control signal, z –output signal, y –measurement signal

For proper process of modelling the norm $\|R(j\omega)\|$ should be as small as possible. The transfer function of the H_∞ controller is given by the following transfer function:

$$H_\infty(s) = \frac{4.4 \cdot 10^5 s^5 + 8.8 \cdot 10^{17} s^4 + 5.4 \cdot 10^{22} s^3 + 4.557 \cdot 10^{25} s^2 + 1.3 \cdot 10^{28} s + 1.6 \cdot 10^{30}}{s^6 + 4.5 \cdot 10^7 s^5 + 5.2 \cdot 10^{12} s^4 + 1.6 \cdot 10^{17} s^3 + 7.3 \cdot 10^{20} s^2 + 7.1 \cdot 10^{22} s + 1.78 \cdot 10^{24}} \quad (15)$$

The frequency responses of the PID closed-loop and the H_∞ closed-loop systems for the uncertainty model of the plant are shown in Fig. 12. The step responses of the PID

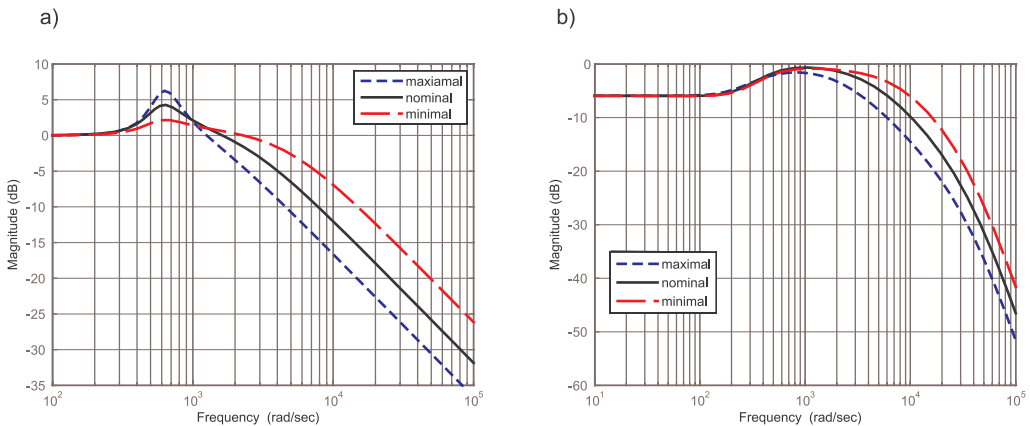


Figure 12. Frequency responses: a) PID closed-loop system, b) H_∞ closed-loop system

closed-loop and H_∞ closed-loop systems for the uncertainty model of the plant are presented in Fig. 13. The H_∞ closed-loop system has shorter settling time and smaller overshoot than the PID closed-loop system. In spite of uncertainties the bandwidth of the H_∞ closed-loop system is much wider than the PID closed-loop system. Because of the weighting functions, the H_∞ closed-loop system has higher order than in the case of the PID closed-loop system.

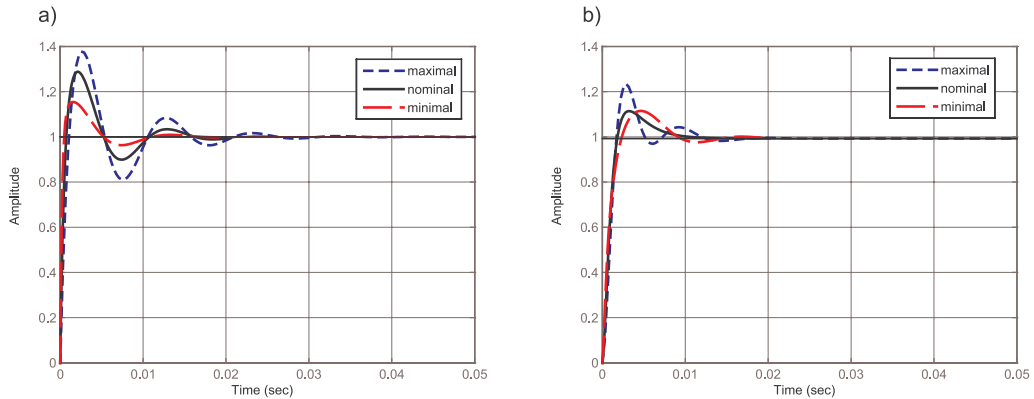


Figure 13. Step responses: a) PID closed-loop system, b) H_∞ closed-loop system

5. Conclusions

In the paper the robust control method was applied in the magnetic bearings system. The uncertainty model of the plant was assigned. We have considered the parametric uncertainty, which was include in the robust control system as additive uncertainty. The input and output signals of the closed-loop system and the disturbances were limited by the weighting functions. The H_∞ robust controller was designed and the H_∞ closed-loop system was investigated. Then PID and H_∞ closed-loop systems were compared. The H_∞ controller achieves better performance than the PID controller. The H_∞ closed-loop system is robust stable in spite of uncertainty. The designed H_∞ closed-loop system assures wide bandwidth up to 1000Hz.

References

- [1] K. ZHOU RM AND J. C. DOYLE: Essentials of robust control. Prentice Hall, 1998.
- [2] K. ZHOU, J.C. DOYLE and K. GLOVER: Robust and optimal control. Prentice Hall, 1997.
- [3] Z. GOSIEWSKI and K. FALKOWSKI: Multifunctional magnetic bearings. Scientific Library of Aviation Institute, Warsaw, 2003.
- [4] J.C. DOYLE, B. FRANCIS and A. TANNENBAUM: Feedback control theory. Macmillan Publishing Co., 1990.
- [5] G.F. FRANKLIN and J. DAVID: Feedback Control of dynamic systems. Prentice Hall, 1997.
- [6] E. LANTTO: Robust control of magnetic bearings in subcritical machines. Dissertation, Helsinki University of Technology, 1999.
- [7] M. ANTILA: Electromechanical properties of radial active magnetic bearings. Dissertation, Helsinki University of Technology, 1998.
- [8] G. BALAS, R. CHIANG, A. PACKARD and A. SAFONOV: Robust control toolbox. MathWorks, 2005.
- [9] A. TEWARI: Modern control design with Matlab and Simulink. Wiley-IEEE Press, 2004.
- [10] R.S. SMITH: Model Validation for robust control: An experimental process control application. University of California, Santa Barbara, 1995.
- [11] T. NAMERIKAWA and M. FUJITA: Uncertainty structure and μ -synthesis of a magnetic suspension system. University of Technology, Kanazawa, T.IEE, **121-C(6)**, (2001).